Constrained Time-lapse Inversion of 3-D Resistivity Surveys Data

Loke, Meng Heng; Dahlin, Torleif; Leroux, Virginie

2011

F06

Constrained Time-lapse Inversion of 3-D Resistivity Surveys Data

M.H. Loke* (Geotomo Software), T. Dahlin (Lund University) & V. Leroux (Lund University)

SUMMARY

Three-dimensional surveys and inversion models are required to accurately resolve structures in areas with very complex geology where 2-D models might suffer from artefacts. 3-D data sets collected at different times are inverted simultaneously using a least-squares methodology that uses roughness filters in both the space and time domains. The spatial roughness filter constrains the model resistivity to vary smoothly in the x, y and z directions. A temporal roughness filter is also applied that minimizes changes in the resistivity between successive temporal inversion models. This method can accurately resolve temporal changes in the resistivity even in the presence of noise. The use of the L1 and L2 norm constraints for the temporal roughness filter are examined using a synthetic model. The L1 norm temporal constraint produces significantly more accurate results when the resistivity changes abruptly with time. A test with field data from a landfill site with methane gas accumulation shows near surface resistivity changes that are probably due to surface temperature variations. The temperature variations cause changes in the gas volume and moisture content in the near surface landfill materials.

Introduction

Two-dimensional resistivity surveys are widely used to map areas with moderately complex geology (Dahlin, 2001). However, in very complex areas, the 2-D inversion model can suffer from artefacts due to structures outside the survey line (Johansson et al., 2007). A 3-D survey and inversion model is required to obtain sufficiently accurate results (Wilkinson et al, 2006; Chambers et al., 2006; Legault et al., 2008). In some areas, repeated 3-D surveys are carried out to detect temporal changes of the subsurface (Rosqvist et al., 2010). In this paper, we adapt the time-lapse inversion methodology by Kim et al. (2009) for 3-D surveys.

Theory

The linearized smoothness-constrained least-squares optimization method is frequently used for 2-D and 3-D inversion of resistivity data (Loke et al., 2003). The 3-D subsurface model used consists of a large number of rectangular cells. The optimization equation that gives the relationship between the model parameters and the measured data is given below.

$$\left[\mathbf{J}_i^T\mathbf{R}_d\mathbf{J}_i + \lambda_i\mathbf{W}^T\mathbf{R}_m\mathbf{W}\right]\Delta\mathbf{r}_i = \mathbf{J}_i^T\mathbf{R}_d\mathbf{g}_i - \lambda_i\mathbf{W}^T\mathbf{R}_m\mathbf{W}\mathbf{r}_{i-1} \quad (1)$$

The Jacobian matrix **J** contains the sensitivities of the measurements with respect to the model parameters, $\boldsymbol{\lambda}$ is the damping factor vector and **g** is the data misfit vector. $\mathbf{r}_{i-1}$ is the model parameter vector (the logarithm of the model resistivity values) for the previous iteration, while is $\Delta\mathbf{r}_i$ is the change in the model parameters. **W** incorporates the roughness filters in the *x*, *y* and *z* directions. $\mathbf{R}_d$ and $\mathbf{R}_m$ are weighting matrices introduced so that different elements of the data misfit and model roughness vectors are given equal weights if the L1-norm inversion method is used (Loke et al., 2003). The inversion methodology by Kim et al. (2009) directly incorporates the time domain with the space domain using the following equation.

$$\left[\mathbf{J}_i^T\mathbf{R}_d\mathbf{J}_i + \lambda_i\left(\mathbf{W}^T\mathbf{R}_m\mathbf{W} + \alpha\mathbf{M}^T\mathbf{R}_t\mathbf{M}\right)\right]\Delta\mathbf{r}_i = \mathbf{J}_i^T\mathbf{R}_d\mathbf{g}_i - \lambda_i\left(\mathbf{W}^T\mathbf{R}_m\mathbf{W} + \alpha_i\mathbf{M}^T\mathbf{R}_t\mathbf{M}\right)\mathbf{r}_{i-1} \quad (2)$$

M is the difference matrix applied across the time models with only the diagonal and one sub diagonal elements having values of 1 and -1, respectively. It minimizes the difference in the resistivity of each model cell and the corresponding cell for the next temporal model. $\boldsymbol{\alpha}$ is the temporal damping factor that gives the relative weight for minimizing the temporal changes in the resistivity compared to the model smoothness and data misfit. Higher values of $\boldsymbol{\alpha}$ will result in time lapsed inverted models that are more similar to one another at the expense of a higher data misfit and model roughness.

Results: Synthetic model test

The test models within a 21 by 16 meters survey grid are shown in Figure 1. The initial model (Figure 1a) has a single high resistivity block of 200 Ω.m in the top layer within a homogeneous medium of 100 Ω.m. In the second time-lapse model (Figure 1b), a moderately high resistivity block of 150 Ω.m is added in the second layer and a low resistivity block of 75 Ω.m in the third layer. The sizes and resistivity contrasts of the blocks of the deeper blocks are increased in the third model (Figure 1c). All the possible dipole-dipole measurements in both the *x* and *y* directions with a geometric factor of less than 1056 m. (that corresponds to a dipole-dipole array with a=1 m. and n=6) are used in the test data set that has 2604 data points. Voltage dependent random noise (Zhou and Dahlin, 2003) with a maximum amplitude of 5% was added to the apparent resistivity values. We used the L1-norm for both the data misfit and model roughness (Loke et al., 2003) in the inversion of the data set. In the first inversion, a L2-norm temporal constraint was used. The third time series inversion model is shown in Figure 2a where all the three blocks are well resolved. The change in the resistivity of the second temporal model compared to the first model is shown in Figure 2b. The inversion model shows changes of +33% and -28% at the locations of the two blocks that are smaller than the actual changes of +50% and -50% in the original model (Figure 1b). The third time series model (Figure 2c) shows changes of +60% and -68% compared to the actual changes of +100% and -100%. The smaller amplitude of the changes in the inversion models is probably partly due to the use of the roughness filters to stabilize the inversion in the presence of noise.

In the second test a L1-norm for the temporal roughness filter is used (Kim et al. 2010). It produces a significant improvement in the models with changes of +40% and -36% for the second times series (actual values of +50% and -50%), and changes of +71% and -76% for the third model (actual values of +100% and -100%). The two deeper blocks are also much better resolved. The 'leakage' of the low resistivity block into the fifth inversion model layer below its true bottom at 1.75 meters depth is much reduced (fifth columns in Figures 2a and 3a). There is a similar reduction in the 'leakage' of the high resistivity anomaly from the second block to the third inversion model layer (third columns in Figures 2c and 3c).

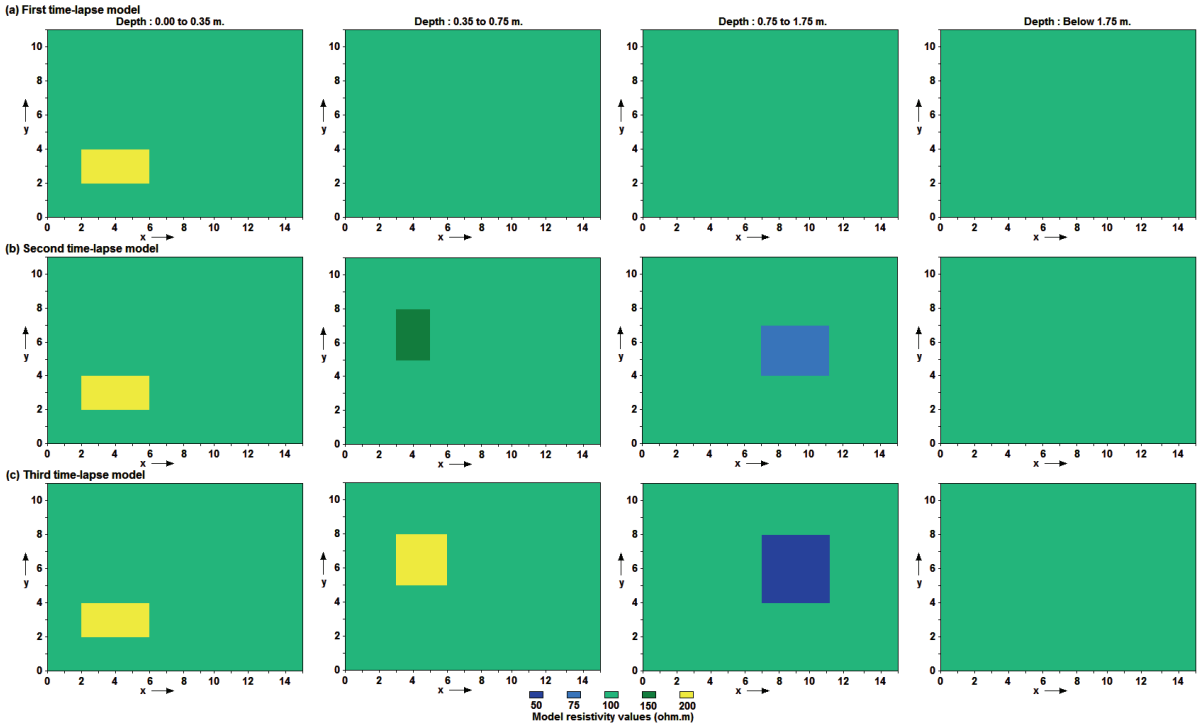

***Figure 1**. The 3-D time-lapse test models.*

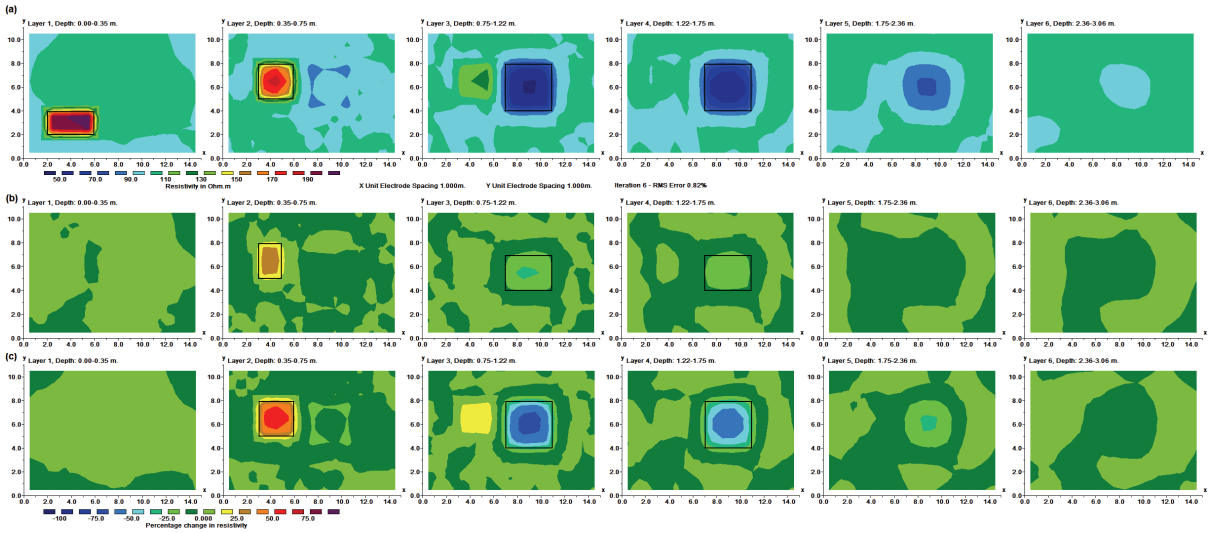

***Figure 2**. Inversion results using L2-norm time-lapse constraint. (a) Third time-lapse inversion model. Percentage change of model resistivity for (b) second and (c) third models compared to first model. The outlines of the true boundaries of the blocks are also shown for comparison.*

Results: Filborna landfill data set

This survey was carried out to map methane gas accumulation in a landfill site at Helsingborg, Sweden (Rosqvist et al., 2010). The survey data set consists of 9 parallel 2-D survey lines with 21

electrodes with a spacing of 1 meter along each line using the pole-dipole array. The spacing between the lines was 2 meters. We used an inversion model with model cells of 1 meter in both horizontal directions, as well as higher damping factors for the first two layers and diagonal roughness filters to reduce banding effects in the inversion (Loke and Dahlin, 2010). The inversion was carried out for two data sets measured on 18th and 27th August 2008 at the same time of the day (about 10 am). The first time series inversion model is shown in Figure 4a. Areas with high methane concentration generally have higher resistivity values. The prominent low resistivity linear feature on the right side of layers 3 and 4 corresponds to a subsurface compost wall consisting of soil and wood chips, while the high resistivity zone above it in layer 1 is believed to be gas that had migrated upwards though the wall. The resistivity difference sections (Figure 4b) show very little variations below a depth of 1.5 meters. There are some minor near surface changes that could be caused by surface temperature variations that cause the gas to contract/expand as the temperature decreases/increases, and also changes in the landfill material moisture content.

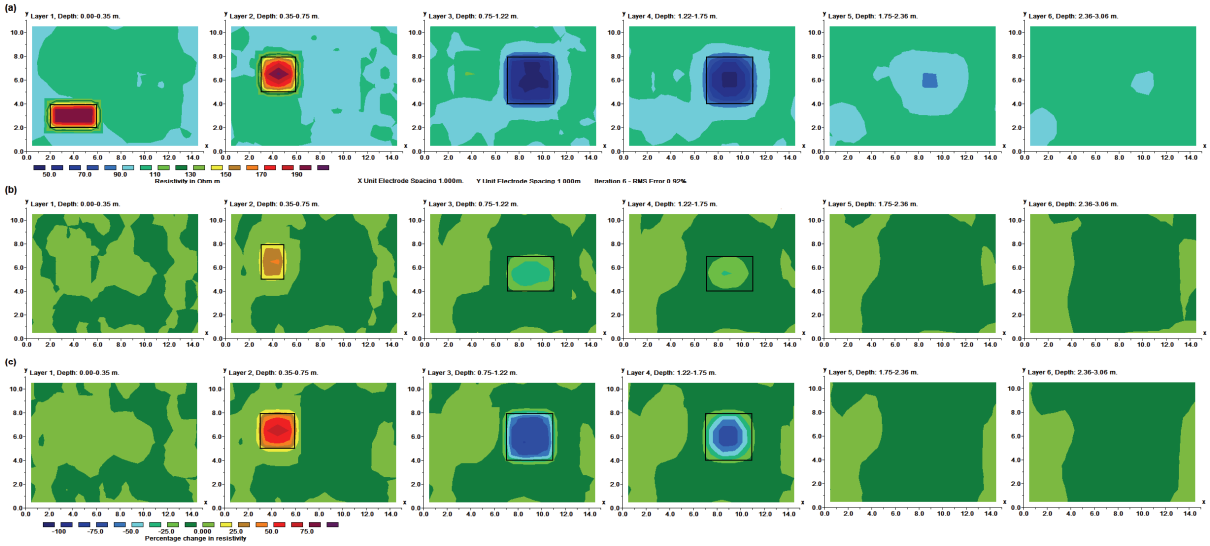

***Figure 3**. Inversion results using L1-norm time-lapse constraint. (a) Third time-lapse inversion model. Percentage change of model resistivity for (b) second and (c) third models compared to first model.*

Conclusion

The constrained time-lapse method can successfully recover temporal changes in the resistivity even in the presence of noise for 3-D resistivity surveys. The L1-norm temporal constraint significantly improves the results when the resistivity changes abruptly with time. An inversion of field data from a landfill site show changes in the resistivity of the materials above 1.5 meters depth. They are probably due to surface temperature variations that cause changes in the methane gas volume and moisture content within the landfill material near the surface.

References

Chambers, J.C., Kuras, O., Meldrum, P.I., Ogilvy, R.D. and Hollands, J., 2006. Electrical resistivity tomography applied to geologic, hydrogeologic, and engineering investigations at a former waste-disposal site. *Geophysics*, **71**, B231-B239.

Dahlin, T., 2001. The development of DC resistivity imaging techniques. *Computers & Geosciences*, **27**, 1019-1029.

Johansson, B., Jones, S., Dahlin, T. and Flyhammar, P., 2007. Comparisons of 2D- and 3D-Inverted Resistivity Data As Well As of Resistivity- and IP-Surveys on a Landfill. *Procs. 13th European Meeting of Environmental and Engineering Geophysics*, Istanbul, Turkey, 3–5 September 2007, P42.

Kim, J H., M J. Yi, S G., Park, and J.G. Kim, 2009. 4-D inversion of DC resistivity monitoring data acquired over a dynamically changing earth model, Journal of Applied Geophysics, **68**, 522-532.

Kim, J.H., 2010. 4-D inversion of resistivity monitoring data using L1 norm minimization. *Procs. 16th European Meeting of Environmental and Engineering Geophysics*, 6 - 8 September 2010, Zurich, Switzerland, A15.

Legault, J.M., Carriere, D. and Petrie, L., 2008. Synthetic model testing and distributed acquisition DC resistivity results over an unconformity uranium target from the Athabasca Basin, northern Saskatchewan. *The Leading Edge*, **27**(1): 46-51.

Loke M.H., Acworth, I. and Dahlin T. 2003. A comparison of smooth and blocky inversion methods in 2D electrical imaging surveys. *Exploration Geophysics*, **34**, 182-187.

Loke, M.H. and Dahlin, T, 2010. Methods to reduce banding effects in 3-D resistivity inversion. *Procs. 16th European Meeting of Environmental and Engineering Geophysics*, 6 - 8 September 2010, Zurich, Switzerland, A16.

Rosqvist, H., Leroux, V., Dahlin,, T., Johansson, S. and Svensson, M., 2010. An evaluation of the potential of the geoelectrical resistivity method for mapping gas migration in landfills. SAGEEP 2010 Proceedings, Keystone, Colorado.

Wilkinson, P.B., Chambers, J.E., Meldrum, P.I., Ogilvy, R.D. and Caunt, S., 2006. Optimization of array configurations and panel combinations for the detection and imaging of abandoned mineshafts using 3D cross-hole electrical resistivity tomography. Journal of Environmental and Engineering Geophysics, **11**, 213-221.

Zhou, B. and Dahlin, T., 2003. Properties and effects of measurement errors on 2D resistivity imaging surveying, Near Surface Geophysics, **1**, 105-117.

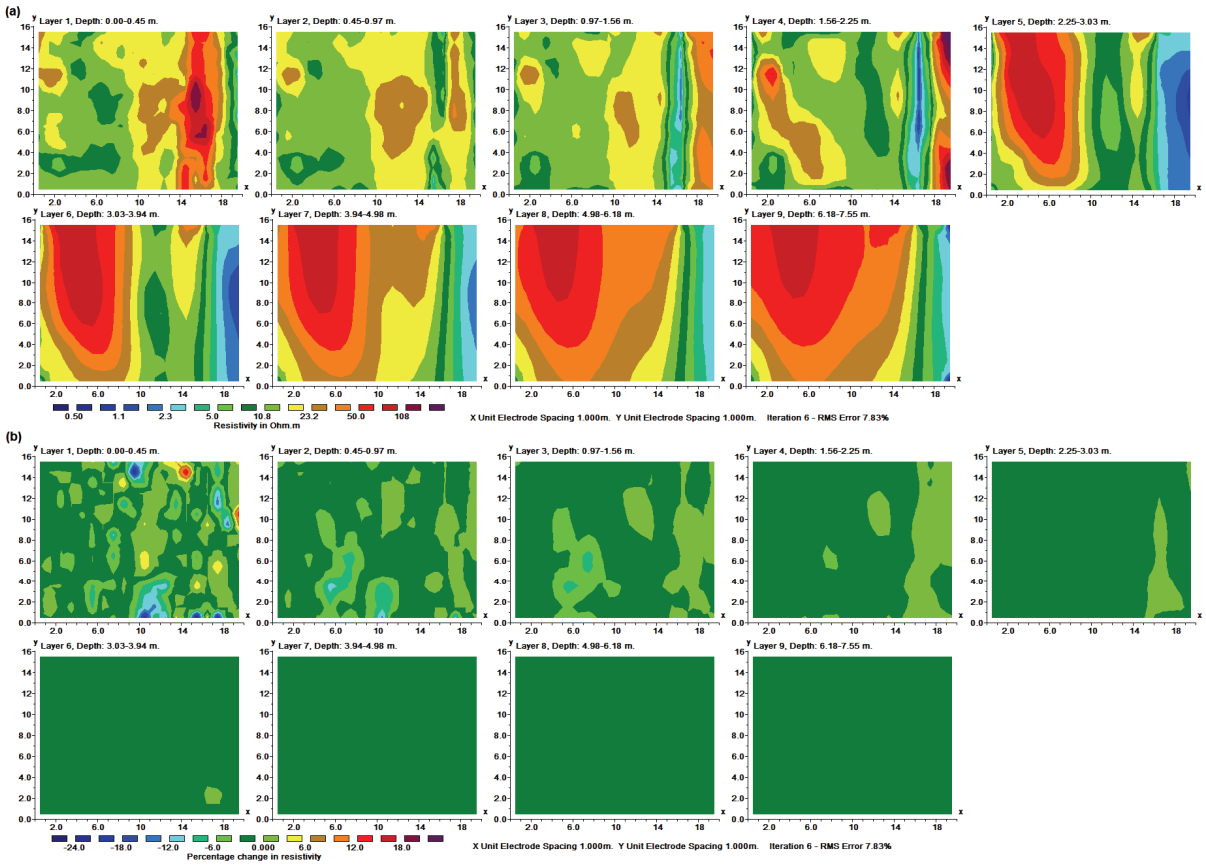

Figure 4. *(a) First time series inversion model for the Filborna landfill survey data set. (b) Change in the resistivity between 18th and 27th August 2008.*